Asynchronism and nonequilibrium phase transitions in (1 + 1)-dimensional quantum cellular automata

Edward Gillman ®,[1,2] Federico Carollo,[3] and Igor Lesanovsky ®[1,2,3]

[1]*School of Physics and Astronomy, University of Nottingham, Nottingham NG7 2RD, United Kingdom*
[2]*Centre for the Mathematics and Theoretical Physics of Quantum Non-Equilibrium Systems, University of Nottingham, Nottingham NG7 2RD, United Kingdom*
[3]*Institut für Theoretische Physik, Universität Tübingen, Auf der Morgenstelle 14, 72076 Tübingen, Germany*

Probabilistic cellular automata provide a simple framework for exploring classical nonequilibrium processes. Recently, quantum cellular automata have been proposed that rely on the propagation of a one-dimensional quantum state along a fictitious discrete time dimension via the sequential application of quantum gates. The resulting (1 + 1)-dimensional space-time structure makes these automata special cases of recurrent quantum neural networks which can implement broad classes of classical nonequilibrium processes. Here, we present a general prescription by which these models can be extended into genuinely quantum nonequilibrium models via the systematic inclusion of *asynchronism*. This is illustrated for the classical contact process, where the resulting model is closely linked to the quantum contact process (QCP), developed in the framework of open quantum systems. Studying the mean-field behavior of the model, we find evidence of an "asynchronism transition," i.e., a sudden qualitative change in the phase transition behavior once a certain degree of asynchronicity is surpassed, a phenomenon we link to observations in the QCP.

Introduction. Nonequilibrium processes can display collective effects and critical behavior. In the vicinity of nonequilibrium phase transitions (NEPTs), the resulting phenomenology can show macroscopic features that are shared by different models. This so-called universality allows for diverse systems to be gathered into few classes, enabling the investigation of emergent phenomena through the analysis of minimal models within a class [1,2]. For classical systems, a paradigmatic setting for exploring nonequilibrium universality is that of (1 + 1)-dimensional cellular automata (CA). These consist of two-dimensional (2D) models realizing an effective 1D system discrete-time dynamics, as shown in Fig. 1(a). The propagation of the 1D state from time t to $t + 1$ occurs through the sequential application of local gates (or rules) operating on the (target) row $t + 1$, controlled by the state of row t; see Fig. 1(a). Such classical dynamics can either be deterministic, usually implemented through unitary gates, or probabilistic, with nonunitary local updates. In the latter case, by suitably choosing the gates, these automata provide discrete-time versions of continuous-time dynamics [1]. Owing to their simple structure, this has allowed for a deep understanding of several classical nonequilibrium processes [1–7].

Recently, quantum versions of these automata have been introduced and dubbed (1 + 1)D quantum cellular automata (QCA) [8–10]. These models are particularly appealing for at least two reasons. First, they can be realized on current quantum simulators [11–14]. Second, while closely linked to unitary 1D QCA [15–19], (1 + 1)D QCA are equivalent to quantum neural networks (QNNs) applied in quantum ma-

chine learning (QML) [20]. In the language of QNNs, the first and last rows of the QCA correspond to input and output layers, respectively, while the intermediate rows are the hidden layers [cf. Fig. 1(a)]. The local gate of the QCA is then a N-input, one-output quantum perceptron, and a quantum evolution proceeds by applying the gate layer by layer, just as in QNNs. Since every perceptron is identical, QCA are in fact recurrent QNNs. With regards to the study of nonequilibrium processes, (1 + 1)D QCA are also particularly effective as they include their classical counterparts as a limiting case, requiring only *synchronous* updates—i.e., commuting gates. For instance, probabilistic cellular automata (PCA) can be reproduced through commuting unitary quantum gates. The QCA state displays nonclassical properties [8,21], but nonetheless captures the classical model, with diagonal elements coinciding with the probabilities of the associated PCA.

In this paper, we present a prescription for extending a given classical model into a genuinely quantum model via the systematic inclusion of *asynchronism* in the (1 + 1)D QCA framework [cf. Fig. 1(b)]. Asynchronism alone is not necessarily a quantum feature [22–24]. However, in QCA, asynchronous—noncommuting—gates can generate a dependence between diagonal observables of one time slice and coherence in the previous one [Fig. 1(c)]. After presenting the general prescription, we analyze the case of the classical *contact process* (CCP). Remarkably, we find that the QCA resulting from the introduction of asynchronism is closely connected to the continuous-time *quantum contact process* (QCP) [25–30]. To make the link precise, we compare the mean-field equations of the QCP and of the asynchronous
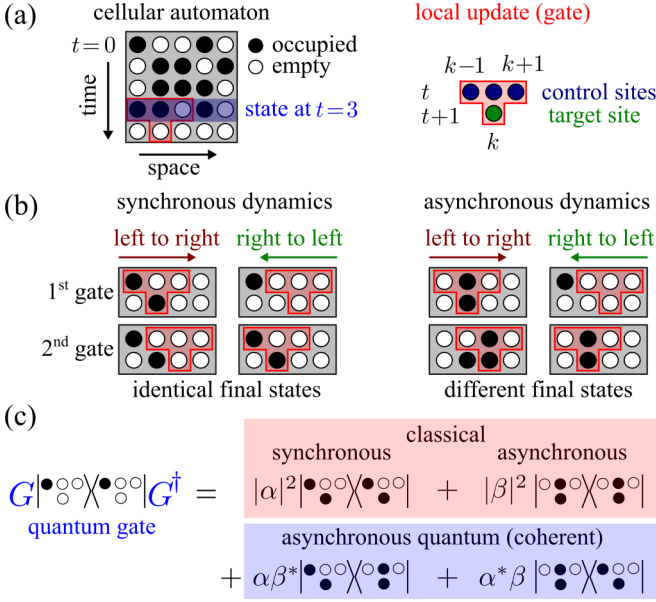
FIG. 1. Asynchronism in classical CA and $(1 + 1)$D QCA. (a) A CA consists of a 2D lattice of two-level systems, which can either be in an occupied or empty state. The vertical dimension of the lattice provides an effective discrete-time dimension and propagation along the time direction is achieved through the sequential application of local gates. These perform operations on a target site at row $t + 1$ and in position k according to the state of three control sites (at position $k - 1, k, k + 1$) in the previous row. After the row $t + 1$ has been completely updated, its state represents the state of an effective 1D system at time $t + 1$. (b) During a single time update, if the local gates do not modify the control sites, the order of their application is irrelevant (synchronous dynamics). If local gates change the control sites, the order of their application is relevant and can produce different final states (asynchronous dynamics). (c) While in a classical CA, the occupation of a target site solely depends on occupation probabilities of control sites, asynchronism in a QCA is linked to quantum coherent processes. In the panel, it is shown how an asynchronous gate can generate, in addition to classical asynchronous terms, a coupling between the occupation in the target site and coherence in the control sites.

QCA. We find that the quantum Hamiltonian contribution in the QCP is analogous to the one due to asynchronism in the QCA. In addition, we investigate the QCA mean-field phase diagram. While for low asynchronism it displays a second-order NEPT in the directed percolation (DP) universality class, as expected from the corresponding PCA [3], there exists a critical value of asynchronism above which the NEPT qualitatively changes and becomes first order. We thus term this an "asynchronism transition." We compare this with the phase diagram estimated using tensor-network techniques and with similar behavior in the QCP.

Our results present a framework to study the role of quantum effects in nonequilibrium collective behavior. Given that noncommuting gates are required for universal computation with qubit-based QNNs [20], our work hints at further interesting links between asynchronism, quantum many-body dynamics, and quantum machine learning.

Synchronous $(1 + 1)$D QCA. In the 2D lattice of the QCA, sites can be in the empty $|\circ\rangle$ or occupied $|\bullet\rangle$ state; see Fig. 1(a). The lattice initial state, $|\psi_0\rangle$, is chosen as a product state, where row $t = 0$ contains the initial 1D configuration, while the other sites are initialized in $|\circ\rangle$. The 2D lattice evolves iteratively as $|\psi_{t+1}\rangle = \mathcal{G}_t |\psi_t\rangle$, where $\mathcal{G}_t$ acts on rows t and $t + 1$. This global update is made of the product of local gates $G_{t,k}$, updating the target site at $(t + 1, k)$. For example, a given ordering could be $\mathcal{G}_t = \ldots G_{t,k} \ldots G_{t,2}G_{t,1}$. The time-evolved 1D system state is $\rho_t = \mathrm{Tr}'(|\psi_t\rangle\langle\psi_t|)$, with the trace taken over all sites except those in row t [cf. Fig. 1(a)]. See Refs. [9,10,21] for further details on $(1 + 1)$D QCA.

The simplest local unitary gate is of the form

$$G_{t,k} = \sum_{\mathcal{N}} P_{\mathcal{N}} \otimes U_{\mathcal{N}}. \tag{1}$$

Here, $\mathcal{N}$ labels the basis states of the "control" sites in the neighborhood of site k on row t. For example, a three-site neighborhood has eight basis states, $\mathcal{N} = (\circ\circ\circ, \circ\circ\bullet, \ldots, \bullet\bullet\bullet)$. The unitary operator $U_{\mathcal{N}}$ "rotates" the target (on row $t + 1$ and in position k) conditioned on the state of the control sites. This is enforced by the projector $P_{\mathcal{N}} = |\mathcal{N}\rangle\langle\mathcal{N}|$ acting on them. We will use the symbol $\otimes$ to separate control sites (to the left) and target sites (to the right). Since in Eq. (1) only orthogonal projectors act on control sites, gates $G_{t,k}$ acting on different target sites commute and the dynamics is synchronous, i.e., target sites can be updated simultaneously [see Fig. 1(b)].

To illustrate that such synchronous $(1 + 1)$D QCA allows for the implementation of a range of canonical nonequilibrium models [4,5,31,32] we consider the realization of the so-called contact process [3,6]. The contact process features three elementary ingredients: decay, i.e., the transition of a site from occupied to empty ($\bullet \rightsquigarrow \circ$), coagulation, which is also the transition of a site from full to empty but facilitated (conditioned) by one of its neighbors ($\bullet\bullet \rightsquigarrow \bullet\circ$), and branching, which is facilitated excitation of the form $\bullet\circ \rightsquigarrow \bullet\bullet$. Note that the contact process possesses the absorbing state $\ldots \circ\circ\circ \ldots$ from which no escape is possible. Whether this state is reached at stationarity depends on the rates (or probabilities) of the elementary processes. An instance of the contact process on a $(1 + 1)$D QCA is realized by the gate

$$G_{t,k} = \Pi_k n_k \otimes U_{\circ\bullet\circ} + \Pi_k \bar{n}_k \otimes \mathbb{1}$$
$$+ \bar{\Pi}_k n_k \otimes U_{\bullet} + \bar{\Pi}_k \bar{n}_k \otimes U_{\circ}, \tag{2}$$

which has the form of Eq. (1). Here $n_k = |\bullet\rangle\langle\bullet|_k$ and $\bar{n}_k = |\circ\rangle\langle\circ|_k = \mathbb{1} - n_k$ project onto the occupied and empty state of site k, respectively. Furthermore, we have defined the projectors $\Pi_k = \bar{n}_{k-1}\bar{n}_{k+1}$ and their complements $\bar{\Pi}_k = \mathbb{1} - \Pi_k$. The unitaries U_α, with labels $\alpha = (\circ\bullet\circ, \bullet, \circ)$, perform a (coherent) flip of the target site, which is conditioned on the state of the controls. Note that the first unitary considers the case of empty left-right control sites, while the latter two unitaries act on the target only if at least one of the left-right control sites is occupied. They are parametrized as $U_{\circ\bullet\circ} = \sqrt{p_{\circ\bullet\circ}} \mathbb{1} - i\sqrt{q_{\circ\bullet\circ}} \sigma^x$ and $U_{\circ/\bullet} = \sqrt{q_{\circ/\bullet}} \mathbb{1} - i\sqrt{p_{\circ/\bullet}} \sigma^x$ with $\sigma^x = |\bullet\rangle\langle\circ| + |\circ\rangle\langle\bullet|$. The parameters $q_{\circ\bullet\circ}$ and $p_{\circ/\bullet} \in [0, 1]$ are the flipping probabilities and $q_\alpha = 1 - p_\alpha$.

In the gate in Eq. (2), the control sites have been separated by singling out the central one, so that we can associate to the target site [in position $(t+1, k)$] a specific control site [the one in position (t, k)], which we regard as its "past." This allows for the mean occupation number, $\langle n_k \rangle_{t+1}$, of the target to be calculated iteratively as

$$\langle n_k \rangle_{t+1} = q_{\circ\bullet\circ} \langle \Pi_k n_k \rangle_t + p_\bullet \langle \bar{\Pi}_k n_k \rangle_t + p_\circ \langle \bar{\Pi}_k \bar{n}_k \rangle_t$$
$$\approx q_{\circ\bullet\circ} \langle \Pi_k \rangle_t \langle n_k \rangle_t + p_\bullet \langle \bar{\Pi}_k \rangle_t \langle n_k \rangle_t + p_\circ \langle \bar{\Pi}_k \rangle_t \langle \bar{n}_k \rangle_t,$$
$$(3)$$

where we performed a mean-field decoupling in the second line [33]. This form makes the interpretation of the probabilities entering the unitaries U_α rather transparent: $q_{\circ\bullet\circ}$ is the probability that the target site k gets occupied given that the control site k is occupied while its neighbors are empty. Since the occupation number can only decrease under this process this effectively implements $\bullet \rightsquigarrow \circ$. The probability $p_\bullet$ is the probability of having an occupied target when there is at least one of the external controls and the central one occupied. This also describes a decay process, but here in combination with the so-called *coagulation process*, i.e., the annihilation of two adjacent occupied sites, e.g., $\bullet\bullet \rightsquigarrow \bullet\circ$. Finally, the probability $p_\circ$ parametrizes the strength of a *branching process* ($\bullet\circ \rightsquigarrow \bullet\bullet$). All these ingredients yield the contact process [6]. Finally, by taking the continuous-time limit of Eq. (3), i.e., expanding $\langle n_k \rangle_{t+1} \approx \langle n_k \rangle_t + \Delta t \frac{d}{dt} \langle n_k \rangle_t$, with small time step Δt, one obtains a continuous-time contact process [6] with coagulation rate $\kappa_c = (q_{\circ\bullet\circ} - p_\bullet)/\Delta t$, branching rate $\kappa_b = p_\circ/\Delta t$, and decay rate $\gamma = p_{\circ\bullet\circ}/\Delta t$ [33].

Asynchronous $(1+1)$D QCA. The dynamics in Eq. (3) is classical as it only connects diagonal observables. A natural question is what is a minimal modification to the gate $G_{t,k}$ which makes diagonal observables at time $t+1$ depend on coherence at the previous time? We achieve this through asynchronism [cf. Figs. 1(b) and 1(c)].

To break the commutativity of the gates, we consider terms modifying control sites along with the target one, see Fig. 1(b), via the gates,

$$G_{t,k} = \sum_{\mathcal{N}} P_{\mathcal{N}} \otimes U_{\mathcal{N}} + \sum_{\mathcal{N} \neq \mathcal{N}'} |\mathcal{N}\rangle\langle\mathcal{N}'| \otimes O_{\mathcal{N},\mathcal{N}'}, \quad (4)$$

where unitarity of $G_{t,k}$ constrains the operators $O_{\mathcal{N},\mathcal{N}'}$. The minimal modification beyond Eq. (1) affects a single control site, i.e., $|\mathcal{N}\rangle\langle\mathcal{N}'| = |\mathcal{N}\rangle\langle\mathcal{N}| \sigma_k^\pm$, where $\sigma^+ = |\bullet\rangle\langle\circ|$ and $\sigma^- = |\circ\rangle\langle\bullet|$, such that

$$G_{t,k} = \sum_{\mathcal{N}} P_{\mathcal{N}} \otimes U_{\mathcal{N}} + \sum_{\mathcal{N},\pm} P_{\mathcal{N}} \sigma_c^\pm \otimes O_{\mathcal{N},\pm}. \quad (5)$$

Here $\sigma_c^\pm$ acts on a chosen site, labeled c. This equation constitutes a prescription for extending any classical model into a quantum one by choosing the operators $O_{\mathcal{N},\pm}$, subject to the constraints of unitarity and any desired physics of the original model.

As an example, we consider the CCP in Eq. (2). In this case, the additional constraints are the presence of the absorbing state and that the update depends only on whether there are any particles present, but not on their quantity or position.
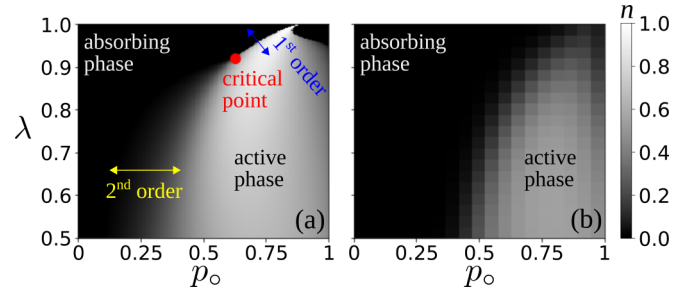

FIG. 2. Nonequilibrium phase transition in $(1+1)$D QCA. (a) Stationary phase diagram for the model described by the gate (6). An absorbing state phase transition is displayed as a function of the asynchronism parameter λ and the branching probability $p_\circ$. The stationary density is estimated by performing 1000 iterations of the mean-field equations [33]. For strong asynchronicity, i.e., $\lambda \gtrsim 0.92$, the phase transition changes from continuous (in the directed percolation universality) to discontinuous. (b) Phase diagram obtained for a $(1+1)$D QCA using tensor networks [21]. Here, the density is calculated using bond dimension $\chi = 64$, lattice size $L = 64$, and by iterating over 100 time steps.

Applying the prescription gives

$$G_{t,k} = \Pi_k n_k \otimes U_{\circ\bullet\circ} + \Pi_k \bar{n}_k \otimes \mathbb{1}$$
$$+ \sqrt{1-\lambda} [\bar{\Pi}_k n_k \otimes U_\bullet + \bar{\Pi}_k \bar{n}_k \otimes U_\circ]$$
$$+ \sqrt{\lambda} \, \bar{\Pi}_k [\sigma_k^+ \otimes U_\bullet U_+ - \sigma_k^- \otimes U_\circ U_+^\dagger]. \quad (6)$$

This gate contains just one additional unitary beyond the synchronous model, $U_+ = i\sqrt{q}\,\mathbb{1} - \sqrt{p}\,\sigma^x$, and features two additional parameters, p and λ, with $\lambda \in [0, 1]$ controlling the strength of the asynchronism. When $\lambda = 0$ we recover Eq. (2). As λ is increased, gates acting on adjacent target sites do not commute, with the norm of the commutator increasing with λ. Considering the analog of Eq. (3) for the gate in Eq. (6), we find after a mean-field decoupling [33]

$$\langle n \rangle_{t+1} = r_{\circ\bullet\circ} \langle \Pi_k \rangle_t \langle n_k \rangle_t + r_\bullet \langle \bar{\Pi}_k \rangle_t \langle n_k \rangle_t + r_\circ \langle \bar{\Pi}_k \rangle_t \langle \bar{n}_k \rangle_t$$
$$+ r_* \langle \bar{\Pi}_k \rangle_t \langle \sigma_k^y \rangle_t, \quad (7)$$

with $\sigma^y = -i\,|\bullet\rangle\langle\circ| + i\,|\circ\rangle\langle\bullet|$. The coefficients are

$$r_{\circ\bullet\circ} = q_{\circ\bullet\circ},$$
$$r_\bullet = (1-\lambda)p_\bullet + \lambda(\sqrt{p_\circ}\sqrt{q} + \sqrt{p}\sqrt{q_\circ})^2,$$
$$r_\circ = (1-\lambda)p_\circ + \lambda(\sqrt{p_\bullet}\sqrt{q} - \sqrt{p}\sqrt{q_\bullet})^2,$$
$$r_* = \sqrt{\lambda}\sqrt{1-\lambda}[\sqrt{q}(p_\bullet + p_\circ)$$
$$+ \sqrt{p}(\sqrt{p_\circ}\sqrt{q_\circ} - \sqrt{p_\bullet}\sqrt{q_\bullet})]. \quad (8)$$

Crucially, we see that this equation connects the density operator n of the target site with the coherence observable σ^y for the central control, which, as mentioned before, we interpret as the "past" of the target. Only when $r_* = 0$ does the equation close on diagonal observables.

Asynchronism transition. To assess the impact of asynchronism on our $(1+1)$D QCA, we investigate the mean-field stationary state [33]. For the following analysis we fix $q_{\circ\bullet\circ} = p_\bullet = p = 0.1$. As shown in Fig. 2(a), for any given value of λ the QCA displays an NEPT from the absorbing state with all empty sites to a state with a finite density of occupied sites,

$\langle n \rangle_\infty \neq 0$. The critical curve separating those two phases can be parametrized by the strength of asynchronism, $\lambda = \lambda_c(p_\circ)$. For $\lambda = 0$ (not shown) the QCA represents a discrete-time contact process and thus shares with it a continuous phase transition in the DP universality class. This continuous transition persists when increasing λ. However, beyond $\lambda^* \approx 0.92$ the phase transition becomes of first order.

Since this change in the nonequilibrium physics occurs for increasing λ along the critical curve λ_c, we call this an "asynchronism transition." This mean-field transition is expected to be strictly observable above the upper-critical dimension of the model. Instead, to study the $(1 + 1)$D QCA, we resort to tensor network methods [21]; see Fig. 2(b). Here, qualitative agreement with the mean-field solution is found, although the NEPT appears to be continuous throughout. Nevertheless, the emergence of the mean-field phase transition may be signaling a changing universality class in the $(1 + 1)$D QCA [33]. As we discuss below, this is analogous to the QCP [28–30], which displays a similar phenomenology.

Relation to the quantum contact process. The QCP is a continuous-time Markovian open quantum system that features the same processes as the CCP, with an additional coherent term known as "quantum branching" ($\bullet\circ \leftrightarrow \bullet\bullet$) with rate Ω [25,26]. This process is implemented by a quantum Hamiltonian, which describes constrained (Rabi) oscillations: sites can only change state when at least one neighbor is occupied. The QCP, as defined in Refs. [25,26], displays a phase transition from an absorbing state to an active phase. At the mean-field level one finds a change of universal behavior from DP to a first-order transition at a certain critical ratio g^* of quantum and classical branching rates, $g = \Omega/\kappa_b$ [25–27]. In 1D, numerical simulations show that the phase transition in fact remains continuous throughout. However, there is still a critical value of g above which one finds deviations from DP universality [28–30]. Thus the QCP displays a change in its universal physics, which, at least at a qualitative level, is indicated by mean field.

The close resemblance between the phenomenology of the QCA (6) and the QCP suggests that the inclusion of asynchronism in the QCA introduces a microscopic process akin to quantum branching [21,25–30,34–36]. To verify this, we consider the Heisenberg equation for n of the QCP [25,26,33]. Upon discretization with time step Δt, this is indeed equivalent to Eq. (7) with coefficients,

$$r_{\circ\bullet\circ} = 1 - \gamma \Delta t, \quad r_\bullet = 1 - \gamma \Delta t - \kappa_c \Delta t,$$
$$r_\circ = \kappa_b \Delta t, \quad r_* = \Omega \Delta t. \tag{9}$$

Comparing Eq. (9) with Eq. (8), we see that removing asynchronism ($\lambda \to 0$) is equivalent to removing coherent branching ($\Omega \Delta t \to 0$) in the QCP.

Finally, we link the asynchronism transition observed previously with similar behavior in the QCP by recharacterizing it in terms of the processes of the QCP. Equating Eqs. (9) and (8), we define the parameter $g = \Omega/\kappa_b$ for our QCA; see
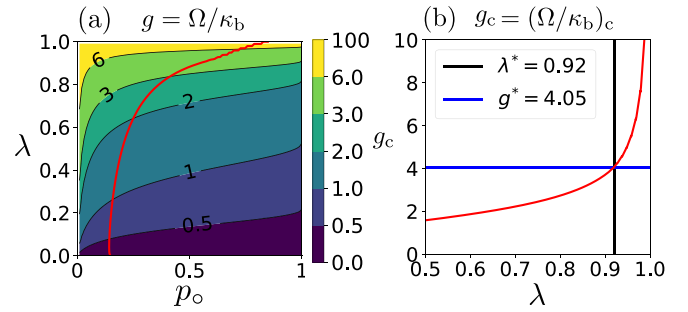

FIG. 3. Quantum and classical processes in asynchronous $(1 + 1)$D QCA. (a) By equating Eqs. (8) and (9), the relative strength of quantum to classical branching, $g = \Omega/\kappa_b$, can be examined for the gate in Eq. (6). As can be seen, g (shown as lines of constant value, with colored areas indicating regions between these values) increases monotonically with the strength of asynchronism in the QCA, parametrized by λ. The solid red line indicates the critical curve of the QCA, estimated by taking the line of constant $n = 0.1$ in the mean-field phase diagram of Fig. 2(a). (b) The behavior of g along the critical line, denoted as g_c here, is shown for $\lambda \in [0.5, 1]$, and displays a rapid increase with λ. The critical point of the asynchronism transition, λ^*, can be identified with a critical value of $g^* = 4.05$.

Fig. 3(a). Clearly, increasing the value of λ corresponds to increasing g. The critical curve, $\lambda = \lambda_c(p_\circ)$, can then also be parametrized by values of g; see Fig. 3(b). In terms of g, the critical point of the asynchronism transition, λ^*, is the point g^*, where quantum branching is sufficiently stronger than classical branching, leading to a change of universal physics in the mean-field phase diagrams and, for 1D QCP, in the (nonperturbative) universality class also.

Conclusion. Building on the connection between classical probabilistic CA and continuous-time nonequilibrium dynamics [3,6], we have demonstrated how asynchronism can be leveraged to gradually introduce genuine quantum effects to an otherwise classical contact process dynamics, and can lead to quantum models that are closely related to those studied in other frameworks. Due to the connection between QCA and QNNs, this analysis might find application in quantum machine learning, for instance, in providing physical insights into the dynamics of information retrieval and the impact of quantum effects—e.g., caused by asynchronism—on their capability of performing computational tasks.

[1] M. Henkel, H. Hinrichsen, and S. Lübeck, *Non-Equilibrium Phase Transitions* (Springer, Netherlands, 2008).

[2] M. Henkel and M. Pleimling, *Non-Equilibrium Phase Transitions* (Springer, Netherlands, 2010).

[3] E. Domany and W. Kinzel, Phys. Rev. Lett. **53**, 311 (1984).

[4] F. Bagnoli, N. Boccara, and R. Rechtman, Phys. Rev. E **63**, 046116 (2001).

[5] F. Bagnoli and R. Rechtman, arXiv:1409.4284.

[6] H. Hinrichsen, Adv. Phys. **49**, 815 (2000).

[7] S. Lübeck, Int. J. Mod. Phys. B **18**, 3977 (2004).

[8] I. Lesanovsky, K. Macieszczak, and J. P. Garrahan, Quantum Sci. Technol. **4**, 02LT02 (2019).

[9] E. Gillman, F. Carollo, and I. Lesanovsky, Phys. Rev. Lett. **125**, 100403 (2020).

[10] E. Gillman, F. Carollo, and I. Lesanovsky, Phys. Rev. A **103**, L040201 (2021).

[11] J. Zeiher, R. Van Bijnen, P. Schauß, S. Hild, J.-y. Choi, T. Pohl, I. Bloch, and C. Gross, Nat. Phys. **12**, 1095 (2016).

[12] H. Kim, Y. J. Park, K. Kim, H.-S. Sim, and J. Ahn, Phys. Rev. Lett. **120**, 180502 (2018).

[13] A. Browaeys and T. Lahaye, Nat. Phys. **16**, 132 (2020).

[14] S. Ebadi, T. T. Wang, H. Levine, A. Keesling, G. Semeghini, A. Omran, D. Bluvstein, R. Samajdar, H. Pichler, W. W. Ho *et al.*, Nature (London) **595**, 227 (2021).

[15] K. Wiesner, Quantum cellular automata, in *Encyclopedia of Complexity and Systems Science*, edited by R. A. Meyers (Springer, New York, 2009), pp. 7154–7164.

[16] J. I. Cirac, D. Perez-Garcia, N. Schuch, and F. Verstraete, J. Stat. Mech. (2017) 083105.

[17] P. Arrighi, Nat. Comput. **18**, 885 (2019).

[18] T. Farrelly, Quantum **4**, 368 (2020).

[19] L. E. Hillberry, M. T. Jones, D. L. Vargas, P. Rall, N. Y. Halpern, N. Bao, S. Notarnicola, S. Montangero, and L. D. Carr, Quantum Sci. Technol. **6**, 045017 (2021).

[20] K. Beer, D. Bondarenko, T. Farrelly, T. J. Osborne, R. Salzmann, D. Scheiermann, and R. Wolf, Nat. Commun. **11**, 808 (2020).

[21] E. Gillman, F. Carollo, and I. Lesanovsky, Phys. Rev. Lett. **127**, 230502 (2021).

[22] O. Bouré, N. Fatès, and V. Chevrier, Nat. Comput. **11**, 553 (2012).

[23] S. Bandini, A. Bonomi, and G. Vizzari, Nat. Comput. **11**, 277 (2012).

[24] N. Fatès, in *Cellular Automata and Discrete Complex Systems*, edited by J. Kari, M. Kutrib, and A. Malcher (Springer, Berlin, 2013), pp. 15–30.

[25] M. Marcuzzi, M. Buchhold, S. Diehl, and I. Lesanovsky, Phys. Rev. Lett. **116**, 245701 (2016).

[26] M. Buchhold, B. Everest, M. Marcuzzi, I. Lesanovsky, and S. Diehl, Phys. Rev. B **95**, 014308 (2017).

[27] D. Roscher, S. Diehl, and M. Buchhold, Phys. Rev. A **98**, 062117 (2018).

[28] F. Carollo, E. Gillman, H. Weimer, and I. Lesanovsky, Phys. Rev. Lett. **123**, 100604 (2019).

[29] E. Gillman, F. Carollo, and I. Lesanovsky, New J. Phys. **21**, 093064 (2019).

[30] M. Jo, J. Lee, K. Choi, and B. Kahng, Phys. Rev. Research **3**, 013238 (2021).

[31] S. Wolfram, Rev. Mod. Phys. **55**, 601 (1983).

[32] S. Wolfram, *A New Kind of Science* (Wolfram Media, Champaign, IL, 2002).

[33] See Supplemental Material at http://link.aps.org/supplemental/10.1103/PhysRevE.106.L032103 for details on the derivation of the mean-field equations presented in the main-text, along with background on the quantum contact process.

[34] M. Jo, J. Um, and B. Kahng, Phys. Rev. E **99**, 032131 (2019).

[35] M. Jo and B. Kahng, Phys. Rev. E **101**, 022121 (2020).

[36] R. Nigmatullin, E. Wagner, and G. K. Brennen, Phys. Rev. Research **3**, 043167 (2021).